frontiers | Frontiers in Environmental Chemistry

TYPE Original Research
PUBLISHED 02 September 2022
DOI 10.3389/fenvc.2022.958607



OPEN ACCESS

EDITED BY
Melissa Ann Maurer-Jones,
University of Minnesota Duluth,
United States

REVIEWED BY
Yan Xia,
Nankai University, China
Mohamed Zbair,
UMR7361 Institut de Sciences des Matériaux de Mulhouse, France

*CORRESPONDENCE
Hélène Budzinski,
helene.budzinski@u-bordeaux.fr

SPECIALTY SECTION
This article was submitted to Organic Pollutants,
a section of the journal
Frontiers in Environmental Chemistry

RECEIVED 31 May 2022
ACCEPTED 20 July 2022
PUBLISHED 02 September 2022

CITATION
Martínez-Álvarez I, Le Menach K, Devier M-H, Cajaraville MP, Orbea A and Budzinski H (2022), Sorption of benzo(a)pyrene and of a complex mixture of petrogenic polycyclic aromatic hydrocarbons onto polystyrene microplastics.
*Front. Environ. Chem.* 3:958607.
doi: 10.3389/fenvc.2022.958607



# Sorption of benzo(a)pyrene and of a complex mixture of petrogenic polycyclic aromatic hydrocarbons onto polystyrene microplastics

Ignacio Martínez-Álvarez[1,2], Karyn Le Menach[1], Marie-Hélène Devier[1], Miren P. Cajaraville[2], Amaia Orbea[2] and Hélène Budzinski[1]*

[1]University of Bordeaux, EPOC-LPTC, UMR 5805 CNRS, Talence Cedex, France, [2]Research Centre for Experimental Marine Biology and Biotechnology PiE and Science and Technology Faculty, CBET research group, Department of Zoology and Animal Cell Biology, University of the Basque Country (UPV/EHU), Leioa, Spain

Microplastics (MPs) largely occur in aquatic ecosystems due to degradation of larger plastics or release from MP-containing products. Due to the hydrophobic nature and large specific surface of MPs, other contaminants, such as polycyclic aromatic hydrocarbons (PAHs), can potentially sorb onto MPs. Several studies have addressed the potential impact of MPs as vectors of PAHs for aquatic organisms. Therefore the role of MPs as sorbents of these compounds should be carefully investigated. The present study aimed to determine the sorption capacity of benzo(a)pyrene (B(a)P), as a model pyrolytic PAH, to polystyrene (PS) MPs of different sizes (4.5 and 0.5 µm). In addition, the sorption of PAHs present in the water accommodated fraction (WAF) of a naphthenic North Sea crude oil to 4.5 µm MPs was also studied as a model of a complex mixture of petrogenic PAHs that could appear in oil-polluted environments. The results indicated that 0.5 µm MPs showed higher maximum sorption capacity ($Q_{max}$) for B(a)P (145–242.89 µg/g) than 4.5 µm MPs (30.50–67.65 µg/g). From the WAF mixture, naphthalene was sorbed at a higher extent than the other PAHs to 4.5 µm MPs but with weak binding interactions ($K_f$ = 69.25 L/g; 1/n = 0.46) according to the analysis of the aqueous phase, whereas phenanthrene showed stronger binding interactions ($K_f$ = 0.24 L/g; 1/n = 0.98) based on the analysis of the solid phase. Sorption of PAHs of the complex WAF mixture to 4.5 µm MPs was relatively limited and driven by the hydrophobicity and initial concentration of each PAH. Overall, the results indicate that sorption estimations based solely on the analysis of the aqueous phase could overestimate the capacity of MPs to carry PAHs. Therefore, controlled laboratory assays assessing the "Trojan Horse effect" of MPs for aquatic organisms should consider these findings in order to design accurate and relevant experimental procedures.

KEYWORDS

**microplastics, polystyrene, sorption, benzo(a)pyrene, competition**

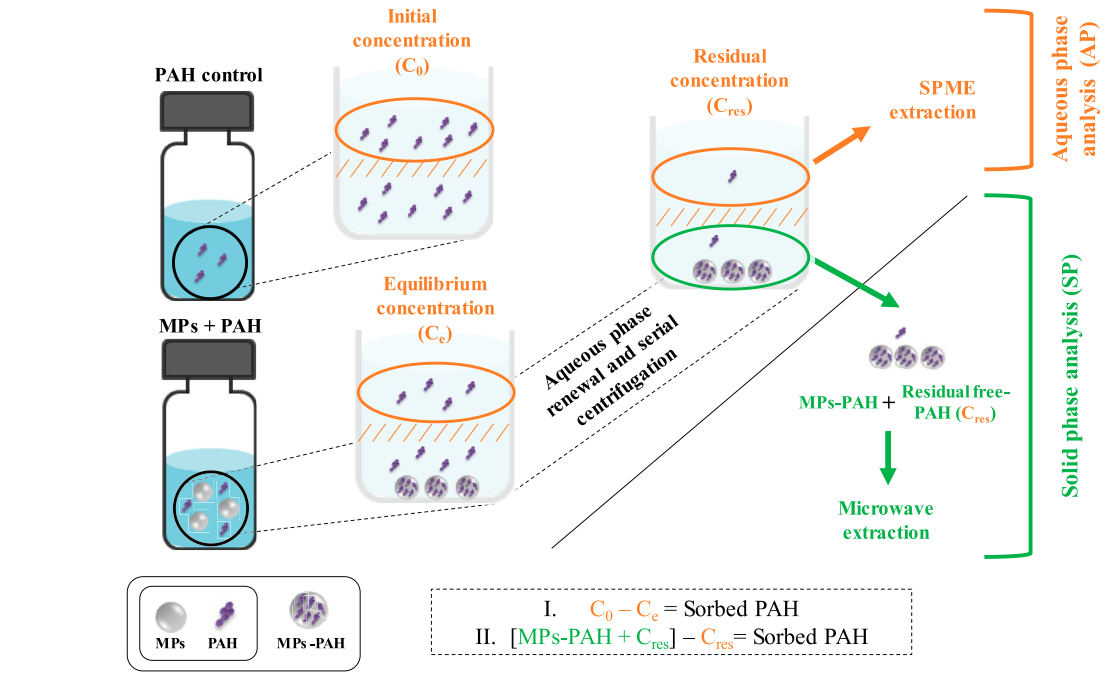


GRAPHICAL ABSTRACT

## Introduction

The widespread use of plastic in consumer products due to their resistance and durability to degradation has become an issue of concern in the recent years. The production of plastics has increased worldwide from 230 million tons in 2005 to 359 million tons in 2018 (Plastics Europe, 2019), leading to an increase in the amount of plastic waste entering aquatic ecosystems, mostly by rivers ending in the oceans (Lebreton et al., 2017). Plastic can be degraded in the environment by physical and chemical processes, producing small plastics known as secondary microplastics (MPs, <5 mm). Plastic is also manufactured to produce small-sized particles (primary MPs) that are incorporated into personal care products and used in industrial applications such as abrasives (Boucher and Friot, 2017). Discharge of these primary MPs during manufacture and use also contributes to the input of small plastic items into the aquatic ecosystems. MPs are reported worldwide in aquatic ecosystems (Chae and An, 2017) at concentrations ranging from 0.002 to 102000 items/$m^3$ for marine ecosystems (Shahul and Hamid, 2018). The most frequent polymers reported in aquatic ecosystems are polyethylene (PE), polypropylene (PP), and PS (Duis and Coors, 2016; Li et al., 2020).

Due to their hydrophobic nature and large specific surface, MPs can sorb persistent organic pollutants (POPs) present in the environment, thus modulating their bioavailability and hazard. Mato et al. (2001) showed the remarkable capacity of plastic resin pellets as a transport medium for POPs in the environment for the first time. Afterward, controlled laboratory experiments investigated the sorption of PAHs to MPs of different composition (Hüffer and Hofmann, 2016; Ma et al., 2016; Wang and Wang, 2018b), as relevant POPs widely distributed on aquatic ecosystems. These experiments show that the properties (density and porosity) of the polymer play an important role in the PAH sorption process and that PS could play an important role as a carrier of POPs. It has also been proven that a larger surface-to-volume ratio of MPs can lead to higher sorption of pollutants present in the water column (Ma et al., 2016; Li et al., 2019; Wang et al., 2019).

Diverse methodologies have been applied to assess the sorption of POPs onto MPs. Extraction is an especially sensitive step due to the potentially damaging effect of the solvents used for extraction on the MPs. For instance, the use of methanol and dichloromethane combined with fluid extraction resulted in a complete dissolution of the MPs (Fuller and Gautam, 2016). A summary of different analytical procedures has been compiled (Rios Mendoza et al., 2017; Skrzypek et al., 2021), showing that gas chromatography-mass spectrometry (GC/MS) is the most suitable analytical technique and that a great variety of solvents and extraction techniques are available. Few studies have undertaken the direct analysis of the PAHs sorbed to MPs (solid phase, SP) due to the aforementioned fragility of MPs (Teuten et al., 2007; Bakir et al., 2012). Most studies estimate the sorption of PAHs by only measuring the

difference in the concentration of the aqueous phase (AP) after MP incubation (Fries and Zarfl, 2012; Ma et al., 2016; Wang and Wang, 2018b; Lin et al., 2019; Wang et al., 2019). However, in order to properly assess the sorption of POPs to MPs in controlled experiments, a methodology that takes into account both phases (Teuten et al., 2007; Reichel et al., 2021) is required.

PAHs are included in the EPA priority pollutant list because of their ubiquitous distribution in the environment and because some members of this chemical class such as benzo(a)pyrene (B(a)P) are prominent and strong carcinogens (Akcha et al., 2003). B(a)P is widely been used in ecotoxicological assays as a model carcinogenic compound, but in the real environment, pollutants do not appear isolated but form complex mixtures and interact with each other. The oil-derived PAHs are also reported as a threat to aquatic organisms (Perrichon et al., 2016), especially the most water-soluble PAHs (naphthalene and phenanthrene) that appear at elevated concentrations in water after spills of many types of oils (Kappell et al., 2014), being therefore the most likely to be present in plastic particles in the environment at places with high pollution pressure (Foshtomi et al., 2019). PAHs behave differently individually or in mixtures toward MPs (Khan et al., 2007; Bakir et al., 2012). The hydrophobicity, solubility of each compound, initial concentration, and presence of co-solutes seem to be relevant factors to take into account for sorption of PAH mixtures to a sorbent (Lamichhane et al., 2016).

The MP's ability to act as carriers of POPs can lead to a phenomenon known as "Trojan Horse effect" (Koelmans et al., 2013; Bakir et al., 2014). MPs with sorbed POPs are susceptible of being ingested by aquatic organisms where those compounds can be released, provoking toxic effects. A large majority of the studies addressing the "Trojan Horse effect" in aquatic organisms are performed using PS microspheres as model MPs (Shen et al., 2019; Strungaru et al., 2019). This is partly explained by the availability of well-characterized and homogeneous particles of a wide range of sizes, especially of small sizes (few microns) and characteristics (i.e., fluorescent, functionalized), manufactured by commercial providers. Therefore, we consider an analysis of the PAH sorption to PS MPs small than 10 µm to be important, which are studied at a lesser extent than larger MPs (Fred-Ahmadu et al., 2020). These small particles are more easily uptaken by a wide range of aquatic organisms. The small size of these particles makes them available for the planktonic species that play a key role in the food chain at the lowest trophic level (Carbery et al., 2018).

The aims of the present work were (I) to assess the sorption capacity of two different sized PS MPs (4.5 and 0.5 µm) for a model pyrolytic PAH of high molecular weight such as B(a)P and (II) to assess the sorption capacity of 4.5 µm PS MPs for PAHs present in the WAF of a naphthenic North Sea (NNS) crude oil, as an environmentally relevant mixture of petrogenic PAHs of low molecular weight. To accomplish these objectives, the two phases of the sorption process were considered: AP, where the free or dissolved PAHs are present, and SP, or MPs, where sorbed PAHs are measured. Modeling of sorption isotherms was applied to estimate the different sorption coefficients in order to compare with previous studies. Herein, the methodologies that have been implemented take into consideration the specificity of MPs concerning chemical analysis (fragility). This work brings new information about partition dynamics between dissolved and SP and in consequence about the sorption mechanisms of PAHs onto MPs. Ultimately, this work aimed to provide the basis for the design of ecotoxicological studies in order to assess the Trojan horse effect of MPs for aquatic organisms.

# Materials and methods

## Materials and chemicals

Aqueous suspensions (2.5% solids, w/v) of PS microspheres 4.5 and 0.5 µm in diameter were purchased from Polysciences, Inc. (Warrington, United States). According to the information provided by the manufacturer, the particles were monodispersed (coefficient of variance < 10%) and inert. Particles presented a glass transition temperature of 95°C, density: 1.05 g/cm$^3$, and a refractive index at 589 nm of 1.59.

B(a)P (purity ≥ 96%), its internal standard (B(a)$P_{d12}$), other 18 deuterated PAHs, and dimethyl sulfoxide (DMSO, purity ≥ 96%) were purchased from Sigma-Aldrich (St. Louis, United States). Unless otherwise specified, other solvents such as methanol (purity ≥ 99.9%) and isooctane (purity ≥ 99.9%) and reagents were also purchased from Sigma-Aldrich. The NNS crude oil was provided by Driftslaboratoriet Mongstad, Equinor (former Statoil).

Conditioned water, used to emulate the sorption process of PAHs to MPs in a real medium for freshwater fish, such as zebrafish, commonly used in ecotoxicology, was prepared from deionized water and commercial salt (SERA, Heinsberg, Germany). The initial pH and conductivity were adjusted to 7–7.5 and 600 µS/cm, respectively.

## Preparation of polycyclic aromatic hydrocarbon solutions

Stocks of 1, 0.1 and 0.01 g/L B(a)P were prepared in 100% DMSO from an initial concentration of 10 g/L. Solutions of 100, 10, and 1 µg/L (0.01% DMSO (v/v) used in the sorption experiments were prepared in deionised water. These concentrations were selected based on previous studies assessing the potential toxicity of MPs combined with PAHs (Batel et al., 2016). Considering GC/MS analyses, solutions of B(a)$P_{d12}$ were prepared in ethanol (2 µg/g) for

solid-phase micro extraction (SPME) or in isooctane for direct injection (2 µg/g). The WAF was prepared following the method of Singer et al. (2000). A small glass bottle was filled with 130 ml of conditioned water and 0.65 g of NNS oil. The bottle was wrapped with aluminum foil and placed in a magnetic stirrer (IKA®-Werke GmbH & Co. KG, Staufen, Germany) at 800 rpm, without vortexing, and 21°C. After 40 h, the AP (100% WAF) was collected, avoiding absorbing oil droplets, and stored at −20°C in a glass bottle until chemical analysis. Dilutions were prepared in conditioned water to obtain 50% and 25% WAF solutions (v/v) for sorption experiments. Solutions of the 18 deuterated PAHs were prepared in ethanol (initial stock solution at 2 µg/g and diluted ones) for SPME/GC/MS analyses and in isooctane (initial stock solution at 8 µg/g and diluted ones) for direct injections.

## Sorption experiments

50 mg/L of MPs of 4.5 and 0.5 µm was incubated (in triplicate) for 24 h in capped aluminum–wrapped glass vials containing 10 ml of 100, 10, or 1 µg/L B(a)P or 100%, 50%, and 25% NNS oil WAF. All materials used in this study were made of glass in order to avoid loss of PAHs due to sorption to other plastic surfaces. Incubation time was also selected according to the literature (Teuten et al., 2007; Batel et al., 2016; Wang and Wang, 2018a). Sorption equilibrium was expected to be reached on the first day of incubation, although it might depend on the polymer and MP size, as well as on studied PAHs (Teuten et al., 2007; Wang and Wang, 2018a). Elevated concentrations (400 mg/L) of several types of polymers [100–250 µm PE, PS, PP, and polyvinyl chloride (PVC)] reached sorption equilibrium for phenanthrene (100 µg/L) between 24 and 48 h of incubation (Teuten et al., 2007; Wang and Wang, 2018a). Thus, a shorter time of equilibrium could be expected for smaller MPs. PAH solutions without MPs (SP) were processed in parallel to monitor the potential (PAH loss due to degradation, sorption onto the vial walls, or to other factors during the experimental procedure). Vials were maintained in an orbital shaker (M1000 VWR, Thorofare, United States) at 300 rpm and 21 ± 1°C in darkness. After incubation, the samples were centrifuged (Hettich Universal 32R centrifuge, Tuttlingen, Germany) at 3,000 g and 4 min for 4.5 µm MPs, and 5,423 g and 45 min for 0.5 µm MPs, according to the manufacturer's instructions. The supernatants were removed and the pellets were washed and resuspended in deionized water and centrifuged again in the same conditions. This step was repeated three times. The supernatants from the 1st (CE1, free PAHs) and 4th (CE4, residual free PAHs) centrifugations were placed in new vials, while supernatants from the 2th and 3th centrifugations were discarded (Supplementary Table S1). All fractions were weighted for mass balance calculation. Then, CE1 samples were diluted up to 1 µg/L according to nominal concentration with deionized water in 10-mL glass SPME vials. SPME consisted of a heating process at 40°C with a 35-min stirring period at 250 rpm of the polydimethylsiloxane (100 µm PDMS) fiber (Supelco, Sigma-Aldrich, South Africa). After extraction, the fiber was thermally desorbed into the GC/MS system (Agilent GC 7890A/Agilent MSD 5975C, Agilent Technology, California) for 10 min at 280°C. The CE4 samples and the pellets containing the MPs were frozen and freeze-dried (Fisher Bioblock Scientific, Illkirch, France) and, then resuspended in methanol (Supplementary Figure S1). PAHs were extracted from MPs by two serial extraction steps of 10 min each by a microwave extraction system (Start E, Milestone, Leutkirch, Germany) in a temperature curve up to 70°C (5 min at 900 W and 5 min at 500 W). Methanol was evaporated with argon gas flux, and the extracts were resuspended in isooctane and further injected in the pulsed splitless injection mode into the GC/MS system. A blank analysis was carried out to ensure the absence of contamination prior to and during analysis. The quality assurance and controls (extraction efficiency, limits of quantification, and control charts) that were carried out are reported in the supporting information (Supplementary Figure S2; Supplementary Tables S2–S4).

## Sorption models

Using the information obtained through the analysis of the AP and of the SP, MP sorption capacity was calculated using two approaches. Values of sorption were expressed as $Q_e$, which is the sorption concentration of the PAH to MPs at equilibrium, and it was calculated as follows for the AP (Eq. 1):

$$Q_e = \frac{(C_0 - C_e)V}{M}, \quad (1)$$

where $C_e$ (µg/L) is the equilibrium concentration in the AP, $C_0$ (µg/L) is the average PAH concentration of the control sample after centrifugation, V (L) is the medium volume, and M (g) is the plastic mass.

For the SP, Eq. 2 was used to calculate Qe values:

$$Q_e = \frac{M_{ext} - C_{res} V_{res}}{M}, \quad (2)$$

where $M_{ext}$ (µg) is the extracted PAH mass, $C_{res}$ (µg/L) is the residual PAH concentration remaining in the AP, $V_{res}$ (L) is the volume of the residual PAH fraction that remained after the last supernatant removal, and M (g) is the plastic mass. In order to evaluate the sorption capacity of the MPs of different sizes for PAHs, the linear, Langmuir, and Freundlich sorption isotherm

TABLE 1 Equations describing the different sorption models and their linear adaptation for graphic representation.

| Model | Equation | Graphic representation of equation |
|---|---|---|
| Linear model | $Q_e = K_d.C_e$ | $Q_e = K_d.C_e$ |
| Langmuir model | $Q_e = Q_{max}.b.C_e/(1 + b.C_e)$ | $1/Q_e = 1/Q_{max} + 1/(b.Q_{max}).1/C_e$ |
| Freundlich model | $Q_e = K_f.C^{e1/n}$ | $\text{Log } Q_e = \log K_f + 1/n.\log C_e$ |

$Q_e$ (μg/g), sorption concentration of PAHs to MPs at equilibrium; $C_e$ (μg/L), equilibrium solution phase concentration of PAHs; $K_d$, partition coefficient of PAH between plastic (MPs) and aqueous phase at equilibrium (L/g); $Q_{max}$, maximum amount of the PAH per weight unit of MPs (μg/g); b, Langmuir constant related to the affinity of binding sites (L/μg); $K_f$, sorption capacity (L/g); 1/n, degree of dependence of sorption at equilibrium.

TABLE 2 B(a)P mass (in ng) in the different measured fractions.

| | Nominal sorption mass | Initial measured mass | | Mass in the aqueous phase (AP, CE1) | Residual mass (AP, CE4) | Sorbed mass (SP) |
|---|---|---|---|---|---|---|
| 4.5 μm | 1000 | 681.00 ± 61.27 | B(a)P control | 665.25 (98%) | - | - |
| | | | MPs-B(a)P | 533.85 ± 58.82 | 0.30 ± 0.22 | 28.11 ± 17.32 |
| | 100 | 52.90 ± 2.39 | B(a)P control | 50.18 (95%) | - | - |
| | | | MPs-B(a)P | 28.73 ± 12.17 | 0.16 ± 0.10 | 6.36 ± 1.42 |
| | 10 | 4.34 ± 0.38 | B(a)P control | 4.33 (100%) | - | - |
| | | | MPs-B(a)P | 2.44 ± 0.43 | <L.Q. | 0.94 ± 0.05 |
| | | | Blank | n.d. | | n.d. |
| 0.5 μm | 1000 | 546.19 ± 34.04 | B(a)P control | 316.71 (58%) | - | - |
| | | | MPs-B(a)P | 48.92 ± 1.63 | 6.33 ± 1.08 | 133.01 ± 35.49 |
| | 100 | 50.76 ± 7.31 | B(a)P control | 34.70 (68%) | - | - |
| | | | MPs-B(a)P | 5.11 ± 0.30 | 0.99 ± 0.48 | 17.93 ± 2.15 |
| | 10 | 4.84 ± 0.68 | B(a)P control | 4.43 (92%) | - | - |
| | | | MPs-B(a)P | 0.39 ± 0.04 | 0.08(*) | 2.50 ± 0.53 |
| | | | Blank | n.d. | | n.d. |

L.Q., limit of quantification (see Supplementary Table S1); n.d., not detected; -, not analyzed; (), recovery percentage from initial mass; *, value obtained from one replicate because the other replicates showed values below L.Q. or not detectable.

models were applied (Table 1) (Yang and Xing, 2010; Wang and Wang, 2018b; Enyoh et al., 2021). A linear adaptation of the Langmuir and Freundlich models was used for graphic representation and parameter acquisition.

# Results and discussion

## Sorption of benzo(a)pyrene to microplastics of different sizes

In the experiments with 4.5 μm MPs, the measured B(a)P mass in initial incubation solutions was lower (68%–43%) than the nominal mass (Table 2). Similar values were obtained in the experiment with 0.5 μm MPs (54%–48%). B(a)P is a highly hydrophobic PAH (water solubility: 1.62 μg/L; ChemIDplus by SRC, 2020). Therefore, in laboratory experiments, DMSO is commonly used as vehicle to increase B(a)P solubility up to 10–50 mg/mL (Keith and Walters, 1991). Nevertheless, transfer of B(a)P from DMSO to a water phase provokes aggregation and precipitation for concentrations higher than its water solubility. Despite these limitations, the selected concentrations allow contaminating MPs in a short time (Wang and Wang, 2018a), which is further needed to perform experiments to assess the potential "Trojan Horse effect" produced by MPs with sorbed PAHs.

B(a)P mass in the control samples varied depending on centrifugation conditions, which, in turn, depended on MP size. Thus, B(a)P control run for the MPs of the two sizes resulted in different recovery values. For 0.5 μm MPs, the increased centrifugation speed and time resulted in a B(a)P recovery of ≈60%–90%, while for 4.5 μm MPs, almost 100%

10.3389/fenvc.2022.958607

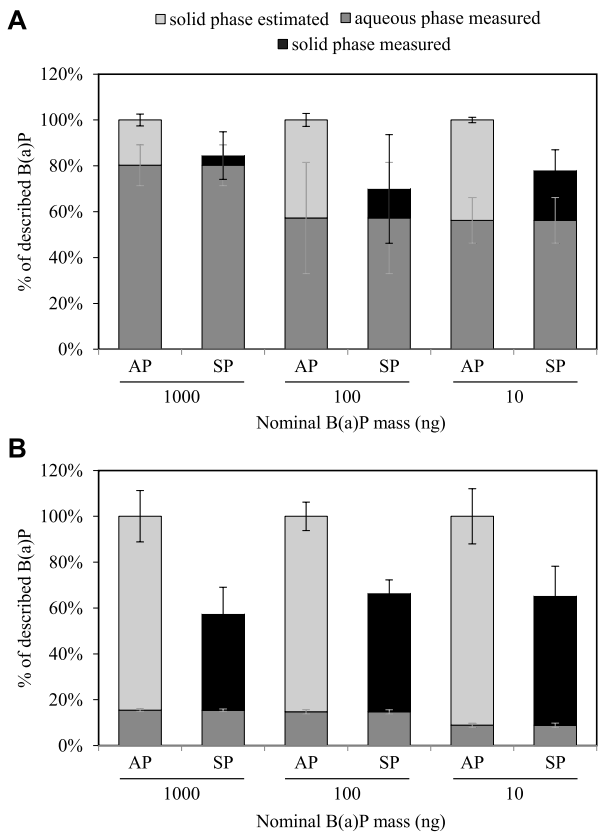


FIGURE 1
Percentage of described B(a)P mass for 4.5 μm MPs **(A)** and for 0.5 μm MPs **(B)** according to measurements carried out in the aqueous phase (AP) or in aqueous and in solid phases (SP).

was recovered. The amount of B(a)P mass in the AP after centrifugation of MPs-B(a)P samples was also lower for 0.5 μm MPs (48.92 ± 1.63 ng) than for 4.5 μm MPs (533.85 ± 58.82 ng) for the highest incubation concentration. The residual mass in the AP (CE4) was less than 20% of the B(a)P control mass and, therefore, almost no interference for SP analysis was assumed. 0.5 μm MP samples showed a higher difference (13%–20.5%) than 4.5 MPs (0%–0.55%) between residual and control samples. Sorbed B(a)P mass measured in SP was higher for 0.5 μm MPs (133.01 ± 35.49, 17.93 ± 2.15, and 2.50 ± 0.53 ng) than for 4.5 μm MPs (28.11 ± 17.32, 6.36 ± 1.42, and 0.94 ± 0.05 ng) at the three sorption concentrations used. Thus, using both AP and SP approaches, the results show that, for the same plastic mass, 0.5 μm MPs are able to sorb a higher amount of B(a)P than 4.5 μm MPs. Previous studies have also proven that a decrease in MP size increases the capacity of sorption of POPs. Batel et al. (2016) analyzed the AP after filtration and found that 1–5 μm fluorescent PS MPs showed higher B(a)P sorption capacity than 10–20 μm PS MPs. A MP size decrease of 4-10 times resulted in a decrease of four times of the total mass of B(a)P found in the AP. In our study, a 10-time decrease of size of PS MPs decreased 10-fold the B(a)P measured mass in the AP.

The percentage of described B(a)P by analyzing one phase (AP) or the two phases (AP and SP) for both MP sizes is shown in Figure 1. Most studies estimate the amount of the sorbed compounds based on the difference in concentration in the initial incubation solution and in the AP after SP separation by filtration (Fries and Zarfl, 2012; Ma et al., 2016; Wang and Wang, 2018b; Lin et al., 2019; Wang et al., 2019). Our results for both MP sizes show that the percentage of B(a)P measured in the SP is markedly lower than the percentage estimated from the measurement of the AP (Figure 1). According to the data obtained only with the analysis of the AP, the 4.5 μm MPs would had sorbed 43% of the B(a)P versus the 13% of B(a)P measured from SP, in the case of MP incubation in the intermediate B(a)P concentration (10 μg/L). For 0.5 μm MPs, the differences in terms of percentage are higher, ranging from 91% of B(a)P sorbed based on the analysis of the AP versus 56% of B(a)P sorbed based on the analysis of the SP, for the lowest initial B(a)P concentration (1 μg/L). As shown by our results and by Teuten et al. (2007), a methodology that includes the analysis of the two phases is the most accurate method for an aqueous-solid sorption phenomenon. These authors evaluated the sorption capacities of polyvinyl chloride, PP, and PE (200–250 μm) for phenanthrene in seawater. The analysis of the AP and SP allowed to explain between 74% (PP) and 85% (PE) of phenanthrene, which is similar to the results obtained in the present study for B(a)P.

The percentage of sorbed B(a)P increases with the decrease of initial B(a)P mass for both MP sizes (Table 2; Figure 1). Wang and Wang (2018b) observed a decrease in the sorption efficiency of phenanthrene to 200–250 μm PS MPs from 55.9% to 32.7% when the initial concentration was increased (0–100 μg/L). On the other hand, the percentage of B(a)P sorbed measured is lower than the expected value for 0.5 μm MPs, with a difference of 20%–40%, and for 4.5 μm MPs with 10%–25% in the three analyzed concentrations. That seems to be related to the total surface area; smaller MPs display a larger total surface area than larger MPs at the same MP concentration. A higher surface means more sorption sites that are potential points of PAH adsorption interactions (hydrophobic and π–π binding interaction) onto the MPs (Fu et al., 2021). These adsorption interactions are more labile than absorption interaction due to the porosity of the material that could account in higher extent for sorbed B(a)P in larger particles (Katsumiti et al., 2019; Lin et al., 2019; Yu et al., 2021). Thus, higher B(a)P desorption could be expected from the small MPs (Fred-Ahmadu et al., 2020) during centrifugation and cleaning.

TABLE 3 PAH mass (in ng) for the different fractions measured.

| | WAF dilution (%) | Initial measured mass | | Mass in the aqueous phase (AP, CE1) | Residual mass (AP, CE4) | Sorbed mass (SP) |
|---|---|---|---|---|---|---|
| Naphthalene | 100 | 2316.55 ± 241.11 | Napht control | 1895.97 (82%) | - | - |
| | | | MPs-Napht | 1617.94 ± 123.06 | 10.51 ± 3.00 | 0.58 ± 0.39 |
| | 50 | 928.39 ± 25.45 | Napht control | 851.09 (92%) | - | - |
| | | | MPs-Napht | 618.84 ± 41.70 | 3.49 ± 1.82 | 0.13 ± 0.06 |
| | 25 | 428.59 ± 11.57 | Napht control | 326.93 (76%) | - | - |
| | | | MPs-Napht | 258.89 ± 15.52# | 2.22 ± 0.47# | 0.12 ± 0.03# |
| | | | Blank | n.d. | | 0.08 |
| Fluorene | 100 | 35.13 ± 1.23 | Fluo control | 31.03 (88%) | - | - |
| | | | MPs-Fluo | 19.21 ± 2.87 | 0.21 ± 0.09 | 0.13 ± 0.07 |
| | 50 | 15.83 ± 0.65 | Fluo control | 13.99 (88%) | - | - |
| | | | MPs-Fluo | 12.32 ± 0.67 | <L.Q. | 0.07* |
| | 25 | 7.91 ± 0.35 | Fluo control | 8.36 (106%) | - | - |
| | | | MPs-Fluo | 5.08 ± 0.012# | <L.Q. | 0.05# |
| | | | Blank | n.d. | | n.d. |
| Phenanthrene | 100 | 24.50 ± 1.68 | Phe control | 13.56 (55%) | - | - |
| | | | MPs-Phe | 11.74 ± 0.90 | 0.17 ± 0.06 | 0.43 ± 0.10 |
| | 50 | 11.16 ± 0.26 | Phe control | 9.29 (83%) | - | - |
| | | | MPs-Phe | 8.19 ± 0.39 | <L.Q. | 0.25 ± 0.07 |
| | 25 | 5.68 ± 0.06 | Phe control | 3.93 (69%) | - | - |
| | | | MPs-Phe | 3.38 ± 0.03# | <L.Q. | 0.24 ± 0.05# |
| | | | Blank | n.d. | | 0.17 |

L.Q., limit of quantification (see Supplementary Table S1); n.d., not detected; -, not analysed; (), recovery percentage from initial mass; #, value obtained from 2 data; *, value obtained from one replicate because the other replicates showed values below L.Q. or not detectable.

## Water accommodated fraction characterization and sorption of polycyclic aromatic hydrocarbons from crude oil water accommodated fraction to 4.5 µm microplastics

The WAF produced from the NNS oil presented a low PAH concentration (ΣPAHs = 300.94 µg/L; Supplementary Table S5) as expected for a low-energy WAF (Singer et al., 2000; Perrichon et al., 2016; Katsumiti et al., 2019). Low-energy WAFs (24 h at 21°C) produced from Arabian Light crude oil (BAL 110) and Erika heavy fuel oil (HFO, no. 2) resulted in similar PAH concentrations, 6.16–170.81 µg/L and 26.10–257.03 µg/L, respectively (Perrichon et al., 2016). Naphthalene (292 µg/L) followed by fluorene and phenanthrene (4.438 and 3.095 µg/L, respectively), were the most abundant PAHs. From the 18 PAHs analyzed, only eight PAHs (the least heavy and hydrophobic ones) were detected in the three WAF dilutions. Thus, the WAF produced from the NNS oil was mostly composed of volatile compounds; the most hydrophobic and potentially toxic compounds were not present or below detection limits.

The naphthalene, fluorene, and phenanthrene masses for the different fractions are shown in Table 3. Only PAHs that appeared in concentrations above quantification limits in the AP and in the SP after the sorption to MPs were analyzed. Measurements in the AP of control samples indicated good recoveries, above 75% in most cases, except for phenanthrene in 25% and 100% WAF. The PAH masses were reduced in the AP for MP-PAH samples compared to control PAH samples for the three studied PAHs. Naphthalene showed the highest decrease in the AP of 100% WAF, from 1895.97 ng to 1617.94 ± 123.06 ng. Fluorene and phenanthrene followed with a mass change from 31.03 ng to 19.21 ± 2.87 ng and from 13.56 ng to 11.74 ± 0.90 ng, respectively. Usually, PAH hydrophobicity (log $K_{ow}$) is the main factor explaining sorption of PAHs to MPs (Hüffer and Hofmann, 2016; Wang and Wang, 2018b). According to this, we expected that phenanthrene (log $K_{ow}$ = 4.46) would be sorbed at the highest extent, followed by fluorene (log $K_{ow}$ = 4.18) and naphthalene (log $K_{ow}$ = 3.30). Nevertheless, in a complex PAH mixture, other factors could be more relevant and should be taken into account to understand the sorption behavior of MPs.

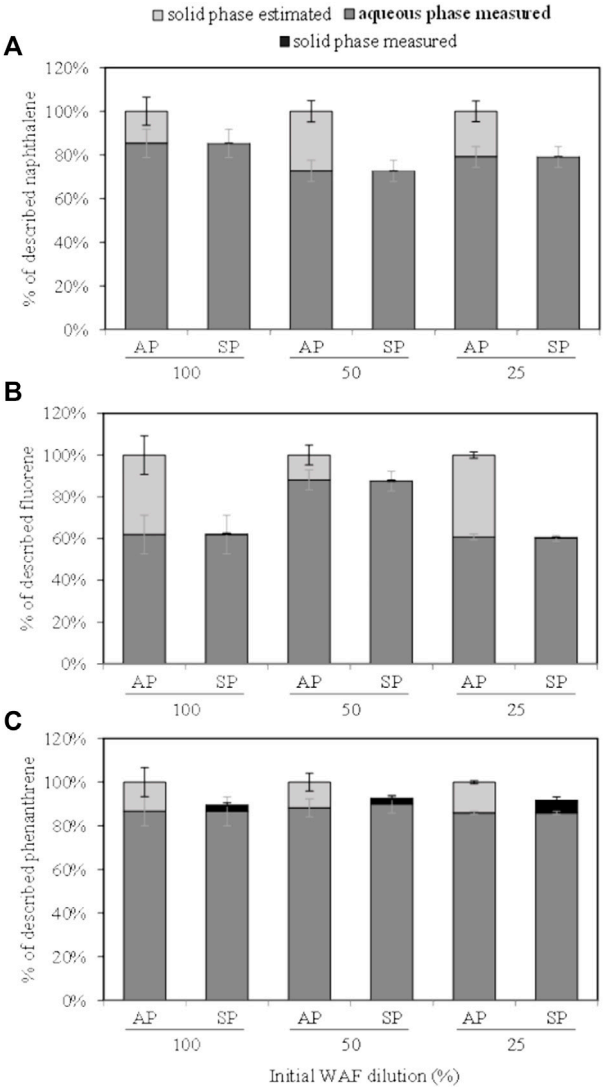


FIGURE 2
Percentage of described PAH mass for naphthalene **(A)**, fluorene **(B)** and phenanthrene **(C)** to 4.5 μm MPs according to measurements done in the aqueous phase (AP) or in aqueous and in solid phases (SP).

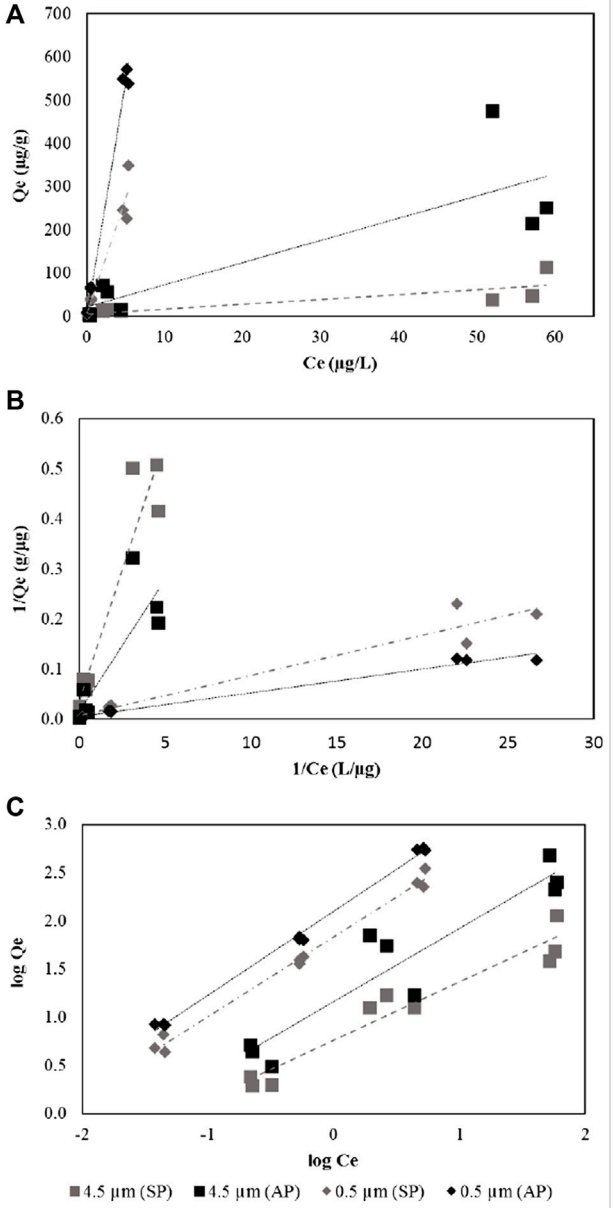


FIGURE 3
Models for the sorption of B(a)P to MPs of different sizes depending on the analyzed fraction (AP and SP). **(A)** Linear model, **(B)** Langmuir model, and **(C)** Freundlich model.

One of these factors is the co-solute phenomenon, as competition among PAHs in the mixture could occur. According to Wang and Wang (2018a), the increase in pyrene concentration (0–20 μg/L) reduces the sorption (partition coefficient, $K_d$) of phenanthrene to PS MPs. In addition, the different ranges of concentrations among PAHs present in the NNS oil WAF (naphthalene was 100 times more concentrated than the other two PAHs) could change the sorption affinity of the different solutes to the sorbent, prioritizing competition for those present at a higher concentration. A favorable sorption scenario has been reported for those PAHs that are present at higher initial concentrations and show a higher affinity for the polymer surface (Bakir et al., 2012; Koelmans et al., 2013; Lamichhane et al., 2016).

After serial centrifugation and AP renewal, the residual mass (CE4) for naphthalene, phenanthrene, and fluorene was under quantification limits or less than 10% of the control sample, indicating almost no interference for the extraction method of the SP. According to the analysis in the SP (Table 3), naphthalene

TABLE 4 Estimated parameters for the Linear, Langmuir, and Freundlich models explaining the sorption of B(a)P to MPs of different sizes, according to data obtained from the aqueous phase (AP) or solid phase (SP).

| MPs | | Linear model | | Langmuir model | | | Freundlich 006D model | | | |
|---|---|---|---|---|---|---|---|---|---|---|
| | | $K_d$ | $R^2$ | $Q_{max}$ | b | $R^2$ | $K_f$ | 1/n | $R^2$ | N |
| 4.5 μm | AP | 5.14 | 0.74 | 67.65 | 0.28 | 0.76 | 14.66 | 0.76 | 0.88 | 9 |
| | SP | 1.13 | 0.71 | 30.50 | 0.31 | 0.91 | 5.77 | 0.61 | 0.93 | 9 |
| 0.5 μm | AP | 108.43 | 0.99 | 242.89 | 0.86 | 0.98 | 125.84 | 0.87 | 1.00 | 9 |
| | SP | 53.57 | 0.95 | 145.00 | 0.86 | 0.95 | 68.60 | 0.83 | 0.99 | 9 |

$K_d$, partition coefficient of B(a)P between MPs and the aqueous phase at equilibrium (L/g); $Q_{max}$, maximum amount of the B(a)P per weight unit of MPs (μg/g); b, Langmuir constant related to the affinity of binding sites (L/μg); $K_f$, sorption capacity (L/g); 1/n, degree of dependence of sorption at equilibrium; $R_2$, linear regression coefficient; N, number of samples.

(0.12–0.58 ng) was the most abundant PAH in the 4.5 μm MPs, followed by phenanthrene, (0.24–0.43 ng) and finally fluorene (0.05–0.13 ng). Those values were close to quantification limits and similar to the values obtained in the blank samples (0.08 ng for naphthalene, 0.17 ng for phenanthrene, and not detected for fluorene). For naphthalene and fluorene, the measured sorbed mass was lower than the residual free mass, suggesting that no sorption occurred to 4.5 μm MPs.

The percentages of the described mass of naphthalene, phenanthrene, and fluorene sorbed to 4.5 μm MPs are shown in Figure 2. Based on the analysis of the AP, differences in the initial PAH concentration did not influence the PAH sorption efficiency, as was seen for B(a)P sorbed to 4.5 μm MPs. Nevertheless, noticeable differences were recorded among compounds. Phenanthrene is more hydrophobic than naphthalene or fluorene and, as a result, it would bind to MPs more strongly than fluorene and naphthalene. However, the higher concentration of naphthalene favors its sorption to MPs, outcompeting the other PAHs. According to the AP analysis in 100% WAF, naphthalene mass sorbed was 278.03 ng versus 11.82 ng and 1.82 ng for fluorene and phenanthrene, respectively. Comparing data for AP and SP analyses, the highly sorbed naphthalene could be desorbed due to cleaning and renewal of the medium. Only the compounds more strongly bound to the MPs, such as phenanthrene, would remain after the process and would then be recovered in the SP analysis.

## Sorption models

In order to analyze the interaction strength and mechanisms of B(a)P sorption to PS MPs, sorption isotherm models were applied from $Q_e$ depending on the analyzed phase and the corresponding $C_e$ values (Figure 3). The corresponding constants and parameters obtained for each model are presented in Table 4. The three models showed linearity, with linear regression coefficients ($R^2$) ranging from 0.71 to 1.00 for the two MP sizes and the two phases analyzed. The models fitted better for 0.5 μm MPs than for 4.5 μm MPs and for the AP than for the SP analysis. Only in the case of 4.5 μm MPs, the SP data fitted better than those of the AP analysis ($R^2$ = 0.91 vs 0.76 for the Langmuir model and 0.93 vs 0.88 for the Freundlich model). According to the linear model, $K_d$ of B(a)P was higher for 0.5 μm MPs than for 4.5 μm MPs with the following order: AP 0.5 μm > SP 0.5 μm > AP 4.5 μm > SP 4.5 μm. Liu et al. (2016) reported Kd values ranging from 38.02 to 177.82 L/g for the sorption of B(a)P to 70 nm PS MPs after 30 days of incubation. Herein, for B(a)P, $K_d$ ranged from 1.13 to 5.14 L/g in the case of 4.5 μm MPs and from 53.57 to 108.43 L/g in the case of 0.5 μm MPs, lower than those reported by Liu et al. (2016), possibly due to the higher MP size. Ma et al. (2016) reported a higher $K_d$ value for the sorption of phenanthrene to 50 nm PS MPs (654 L/g) than to 10 μm PS MPs (16.9 L/g) after 7 days of incubation. Wang and Wang (2018b) also analyzed sorption of phenanthrene to 200–250 μm PS MPs and estimated a partition coefficient of 1.861 L/g. Thus, our results agree with previously published data regarding PAH partition coefficient and MP size: the higher the MP size, the lower the partition coefficient.

TABLE 5 Estimated parameters of the Freundlich model for WAF PAH sorption to 4.5 μm MPs, according to data obtained from the aqueous phase (AP) or solid phase (SP).

| PAH | Log $K_{ow}$ | | $K_f$ | 1/n | $R^2$ | N |
|---|---|---|---|---|---|---|
| Naphthalene | 3.36 | AP | 69.25 ± 32.68 | 0.46 | 0.36 | 8 |
| | | SP | — | — | — | — |
| Fluorene | 4.18 | AP | 10.82 ± 7.85 | 0.70 | 0.16 | 8 |
| | | SP | 0.12 ± 0.02 | -0.29 | 0.48 | 3 |
| Phenanthrene | 4.46 | AP | 3.28 ± 1.22 | 0.63 | 0.51 | 8 |
| | | SP | 0.24 ± 0.16 | 0.98 | 0.32 | 7 |

$K_f$, sorption capacity of MPs for PAHs (L/g); 1/n, degree of dependence of sorption at equilibrium; $R^2$, linear regression coefficient; N, number of samples.

The results of the Langmuir model based on the analysis of the AP indicated that 0.5 µm MPs showed a higher $Q_{max}$ for B(a)P than 4.5 µm MPs: $Q_{max}$ of 242.89 µg/g and 67.65 µg/g for 0.5 µm MPs and 4.5 µm MPs, respectively. Wang and Wang (2018a) reported a Qmax value of 127 µg/g using a range of pyrene concentrations from 0 to 100 µg/L to assess sorption to 100–150 µm PS MPs (200 mg/L) after 48 h of incubation. This value was similar to the value we calculated for 4.5 µm MPs and lower than the value for 0.5 µm MPs likely due to the higher concentration of PS MPs used and the lower hydrophobicity of pyrene (log $K_{ow}$ = 4.88) in comparison to B(a)P (log $K_{ow}$ = 6.35). The b independent coefficient indicates the sorption nature between the sorbate and the sorbent, being unfavorable if b > 1, linear if b = 1, favorable if 0 < b < 1, or irreversible if b = 0 (Zhan et al., 2016). The b independent coefficient showed values of 0.86 L/µg for 0.5 µm MPs and 0.28–0.31 L/µg for 4.5 MPs (Table 4), indicating a more favorable sorption of B(a)P for 0.5 µm MPs than for 4.5 µm MPs.

For MPs of both sizes, the Freundlich model fitted better than the Langmuir model. The Freundlich model describes the formation of a sorbate monolayer by assuming that the adsorption occurs on a homogenous surface and there are no interferences between different sorbates (Yang and Xing, 2010). In agreement with previous data, the affinity of the sorbate to the sorbent ($K_f$) was higher for 0.5 µm MPs than for 4.5 µm MPs, being 125.84 and 14.66 L/g respectively, based on the analysis of the AP. Liu et al. (2016) reported a nonlinear sorption tendency of B(a)P to 70 nm PS nanoparticles with a $K_f$ value of 33884.41 L/g. In the present study, 10 times smaller MPs resulted in an almost 10-fold increase in $K_f$ value according to the analysis of the AP and a 13-fold increase in $K_f$ value according to the analysis of the SP. The coefficient "1/n" allows knowing whether the adsorption is cooperative (1/n < 1; Bakir et al., 2014; Hüffer and Hofmann, 2016). The results indicate that cooperation was also higher for 0.5 µm MPs (1/n = 0.87 for AP analysis and 1/n = 0.83 for SP analysis) than for 4.5 µm MPs (1/n = 0.76 for AP analysis and 1/n = 0.61 for SP analysis). 1/n values close to 1 seem to be related to sorption by partitioning into the PS MPs rather than to adsorption onto the polymer surface. In the study by Wang et al. (2019), sorption of phenanthrene to PS MPs of 50 nm–170 µm ranged from 100 to 80 µg/L, the cooperation was up to 0.79 for 170 µm PS MPs and 0.95 for 50 nm MPs, indicating that cooperation increased with the MP size. Higher B(a)P sorption capacity and sorption affinity for 0.5 µm MPs than for 4.5 µm MPs was confirmed.

Isotherms for the three PAHs analyzed in the NNS crude oil WAF and 4.5 µm MP experiments were nonlinear (Supplementary Figure S3) for both analyzed phases. Values of the linear regression coefficients ($R^2$) for the Freundlich model ranged from 0.16 to 0.51 (Table 5). This nonlinearity suggests PAH binding onto the surface of the MPs and no correlation between initial PAH concentration and the amount of PAHs sorbed to MPs (similar sorption values for the three WAF dilutions used). PAHs that are poorly bound to the sorbent can also be lost during the sample processing. Despite the nonlinear tendency shown by the models, average $K_f$ was calculated. Naphthalene showed the highest $K_f$ value (69.25 L/g), followed by fluorene (10.82 L/g) and finally phenanthrene (3.28 L/g) according to the analysis of the AP (Table 5). But opposite to $K_f$ values, 1/n coefficients showed higher sorption cooperation for fluorene (0.70) and phenanthrene (0.63), with similar octanol/water partition coefficients, than for naphthalene (0.46). Few authors have addressed the sorption of naphthalene to MPs. Hüffer and Hofmann (2016) reported that naphthalene was the compound that sorbed least to different polymers, only followed by benzene. Karapanagioti et al. (2010) observed that naphthalene was the first PAH (before pyrene and phenanthrene) to reach sorption equilibrium with PE and PP pellets. In addition, naphthalene is a small PAH that tends to interact with MPs by "hole-filling" (Khan et al., 2007). Naphthalene can outcompete with heavier PAHs for adsorption to the material surface.

Naphthalene sorption to MPs could not be assessed in the SP because a higher naphthalene concentration was found in the residual fraction than in the SP. From the analysis of the SP, phenanthrene showed higher $K_f$ (0.24 L/g) and 1/n coefficients (0.98) than fluorene ($K_f$ = 0.12 L/g; 1/n = −0.29). Phenanthrene is one of the most studied PAHs regarding sorption to MPs (Bakir et al., 2014; Liu et al., 2016; Ma et al., 2016; Wang and Wang, 2018b). Bakir et al. (2014) assessed PE MPs (200–250 µm) for 1,1′-(2,2,2-trichloroethane-1,1-diyl)bis(4-chlorobenzene) (DDT) and phenanthrene sorption affinity at the same range of concentrations (0.2–6.1 µg/L). They reported more affinity for the most hydrophobic compound (DDT), with $K_f$ values of 794.3 L/g and 79.43 L/g for DDT and phenanthrene, respectively. Fries and Zarfl (2012) showed that sorption values to PE MPs were lower for fluorene than for phenanthrene, with $K_d$ values of 8 L/Kg and 19 L/Kg, respectively, reinforcing the idea that sorption was closely related to the log $K_{ow}$ of the analyzed PAHs.

## Conclusion

In conclusion, the present study shows that a methodology for the assessment of PAH sorption to MPs based on the analysis of both, aqueous and solid phases, provides information that helps understand the interaction and mechanisms of sorption of PAHs to MPs of different sizes. The results show that the estimated amount of sorbed compounds to MPs is usually overestimated if based only on the analysis of the aqueous phase. 0.5 µm MPs were found to sorb higher amounts of B(a)P than 4.5 µm MPs, indicating that size is a key parameter influencing the role of MPs as carriers of organic pollutants. At complex environmental conditions, as those that can reflect the PAH mixture present

in a naphthenic crude oil WAF, PAH sorption to 4.5 μm MPs is mainly driven by PAH hydrophobicity and initial PAH concentration. Moreover, competition among PAHs for the binding sites of MPs results in complex interactions between PAHs and MPs. Further studies with MPs of different sizes and other organic pollutants at environmentally relevant conditions would help characterize the risk posed by MPs as vectors of pollutants for aquatic ecosystems.

## Data availability statement

The original contributions presented in the study are included in the article/Supplementary Material; further inquiries can be directed to the corresponding author.

## Author contributions

Conceptualization, HB and AO; methodology, IM-A and KL; software, IM-A; validation, KL, HB, and AO; formal analysis, IM-A; investigation, IM-A; resources, KL, M-HD, and AO; writing—original draft preparation, IM-A; writing—review and editing, AO, M-HD, HB, and MC.; visualization, IM-A and AO; supervision, HB and AO; project administration, M-HD, MC, HB, and AO; funding acquisition, MC, HB, and AO. All authors have read and agreed to the final version of the manuscript.

## Funding

Funded by Spanish MINECO (NACE project—CTM 2016-81130-R), Basque Government (consolidated research group IT810-13 and IT1302-19), UPV/EHU (UFI 11/37 and grant to IMA) and French ANR (No. –10–IDEX-03-02 and Cluster of Excellence COTE (ANR-10-LABX 45).

## Acknowledgments

We thank the staff at Driftslaboratoriet Mongstad Equinor (former Statoil) for supplying the crude oil used in the experiments.

## Conflict of interest

The authors declare that the research was conducted in the absence of any commercial or financial relationships that could be construed as a potential conflict of interest.

## Publisher's note

All claims expressed in this article are solely those of the authors and do not necessarily represent those of their affiliated organizations, or those of the publisher, the editors, and the reviewers. Any product that may be evaluated in this article, or claim that may be made by its manufacturer, is not guaranteed or endorsed by the publisher.

## Supplementary material

The Supplementary Material for this article can be found online at: https://www.frontiersin.org/articles/10.3389/fenvc.2022.958607/full#supplementary-material

## References

Akcha, F., Burgeot, T., Narbonne, J-F., and Garrigues, P. (2003). *Metabolic activation of PAHs: Role of DNA adduct formation in induced carcinogenesis" in PAHs: An ecotoxicological perspective*. West Sussex, England): John Wiley & Sons, 65–80.

Bakir, A., Rowland, S. J., and Thompson, R. C. (2014). Enhanced desorption of persistent organic pollutants from microplastics under simulated physiological conditions. *Environ. Pollut.* 185, 16–23. doi:10.1016/j.envpol.2013.10.007

Bakir, A., Rowland, S. J., and Thompson, R. C. (2012). Competitive sorption of persistent organic pollutants onto microplastics in the marine environment. *Mar. Pollut. Bull.* 64, 2782–2789. doi:10.1016/j.marpolbul.2012.09.010

Batel, A., Linti, F., Scherer, M., Erdinger, L., and Braunbeck, T. (2016). Transfer of benzo[a]pyrene from microplastics to artemia nauplii and further to zebrafish via a trophic food web experiment: cyp1a induction and visual tracking of persistent organic pollutants. *Environ. Toxicol. Chem.* 35, 1656–1666. doi:10.1002/etc.3361

Boucher, J., and Friot, D. (2017). *Primary microplastics in the oceans: A global evaluation of sources*. Gland, Switzerland): IUCN, 1–43.

Carbery, M., O'Connor, W., and Thavami, P. (2018). Trophic transfer of microplastics and mixed contaminants in the marine food web and implications for human health. *Environ. Int.* 115, 400–409. doi:10.1016/j.envint.2018.03.007

Chae, Y., and An, Y. (2017). Effects of micro- and nanoplastics on aquatic ecosystems: Current research trends and perspectives. *Mar. Pollut. Bull.* 124, 624–632. doi:10.1016/j.marpolbul.2017.01.070

ChemIDplus by SRC (2021). Inc. Available at: http://chem.sis.nlm.nih.gov/chemidplus/name/benzo(a)pyrene (accessed Jan 20, 2021).

Duis, K., and Coors, A. (2016). Microplastics in the aquatic and terrestrial environment: Sources (with a specific focus on personal care products), fate and effects. *Environ. Sci. Eur.* 28, 2–25. doi:10.1186/s12302-015-0069-y

Enyoh, C. E., Ohiagu, F. O., Verla, A. W., Qingyu, W., Shafea, L., Verla, E. N., et al. (2021). 'Plasti-remediation": Advances in the potential use of environmental plastics for pollutant removal. *Environ. Technol. Innov.* 23, 101791. doi:10.1016/j.eti.2021.101791

Foshtomi, M. Y., Oryan, S., Taheri, M., Bastami, K. D., and Zahed, M. A. (2019). Composition and abundance of microplastics in surface sediments and their interaction with sedimentary heavy metals, PAHs and TPH (total petroleum hydrocarbons). *Mar. Pollut. Bull.* 149, 110655. doi:10.1016/j.marpolbul.2019.110655

Fred-Ahmadu, O. H., Bhagwat, G., Oluyoye, I., Benson, N. U., Ayejuyo, O. O., and Palanisami, T. (2020). Interaction of chemical contaminants with microplastics:

Principles and perspectives. *Sci. Total Environ.* 706, 135978. doi:10.1016/j.scitotenv.2019.135978

Fries, E., and Zarfl, C. (2012). Sorption of polycyclic aromatic hydrocarbons (PAHs) to low and high density polyethylene (PE). *Environ. Sci. Pollut. Res.* 19, 1296–1304. doi:10.1007/s11356-011-0655-5

Fu, L., Li, J., Wang, G., Luan, Y., and Dai, W. (2021). Adsorption behavior of organic pollutants on microplastics. *Ecotoxicol. Environ. Saf.* 217, 112207. doi:10.1016/j.ecoenv.2021.112207

Fuller, S., and Gautam, A. (2016). A procedure for measuring microplastics using pressurized fluid extraction. *Environ. Sci. Technol.* 50, 5774–5780. doi:10.1021/acs.est.6b00816

Hüffer, T., and Hofmann, T. (2016). Sorption of non-polar organic compounds by micro-sized plastic particles in aqueous solution. *Environ. Pollut.* 214, 194–201. doi:10.1016/j.envpol.2016.04.018

Kappell, A. D., Wei, Y., Newton, R. J., Van Nostrand, J. D., Zhou, J., McLellan, S. L., et al. (2014). The polycyclic aromatic hydrocarbon degradation potential of Gulf of Mexico native coastal microbial communities after the Deepwater Horizon oil spill. *Front. Microbiol.* 5, 205. doi:10.3389/fmicb.2014.00205

Karapanagioti, H., Ogata, Y., and Takada, H. (2010). Eroded plastic pellets as monitoring tools for polycyclic aromatic hydrocarbons (PAH): Laboratory and field studies. *Glob. NEST J.* 12, 327–334.

Katsumiti, A., Nicolussi, G., Bilbao, D., Prieto, A., Etxebarria, N., and Cajaraville, M. P. (2019). *In vitro* toxicity testing in hemocytes of the marine mussel *Mytilus galloprovincialis* (L.) to uncover mechanisms of action of the water accommodated fraction (WAF) of a naphthenic North Sea crude oil without and with dispersant. *Sci. Total Environ.* 670, 1084–1094. doi:10.1016/j.scitotenv.2019.03.187

Keith, L. H., and Walters, D. B. (1991). *National Toxicology program's chemical solubility database*. Chelsea, USA: Lewis Publishers.

Khan, E., Khaodhir, S., and Rotwiron, P. (2007). Polycyclic aromatic hydrocarbon removal from water by natural fiber sorption. *Water Environ. Res.* 79, 901–911. doi:10.2175/106143007x176040

Koelmans, A. A., Besseling, E., Wegner, A., and Foekema, E. M. (2013). Plastic as a carrier of POPs to aquatic organisms: A model analysis. *Environ. Sci. Technol.* 47, 7812–7820. doi:10.1021/es401169n

Lamichhane, S., Bal Krishna, K. C., and Sarukkalige, R. (2016). Polycyclic aromatic hydrocarbons (PAHs) removal by sorption: A review. *Chemosphere* 148, 336–353. doi:10.1016/j.chemosphere.2016.01.036

Lebreton, L. C. M., Zwet, J., Damsteeg, J., Slat, B., Andrady, A., and Reisser, J. (2017). River plastic emissions to the world's oceans. *Nat. Commun.* 8, 15611. doi:10.1038/ncomms15611

Li, C., Busquets, R., and Campos, L. C. (2020). Assessment of microplastics in freshwater systems: A review. *Sci. Total Environ.* 707, 135578. doi:10.1016/j.scitotenv.2019.135578

Li, Y., Li, M., Li, Z., Yang, L., and Liu, X. (2019). Effects of particle size and solution chemistry on Triclosan sorption on polystyrene microplastic. *Chemosphere* 231, 308–314. doi:10.1016/j.chemosphere.2019.05.116

Lin, W., Jiang, R., Wu, J., Wei, S., Yin, L., Xiao, X., et al. (2019). Sorption properties of hydrophobic organic chemicals to micro-sized polystyrene particles. *Sci. Total Environ.* 690, 565–572. doi:10.1016/j.scitotenv.2019.06.537

Liu, L., Fokkink, R., and Koelmans, A. A. (2016). Sorption of polycyclic aromatic hydrocarbons to polystyrene nanoplastic. *Environ. Toxicol. Chem.* 35, 1650–1655. doi:10.1002/etc.3311

Ma, Y., Huang, A., Cao, S., Sun, F., Wang, L., Guo, H., et al. (2016). Effects of nanoplastics and microplastics on toxicity, bioaccumulation, and environmental fate of phenanthrene in fresh water. *Environ. Pollut.* 219, 166–173. doi:10.1016/j.envpol.2016.10.061

Mato, Y., Isobe, T., Takada, H., Kanehiro, H., Ohtake, C., and Kaminuma, T. (2001). Plastic resin pellets as a transport medium for toxic chemicals in the marine environment. *Environ. Sci. Technol.* 35, 318–324. doi:10.1021/es0010498

Perrichon, P., Le Menach, K., Akcha, F., Cachot, J., Budzinski, H., and Bustamante, P. (2016). Toxicity assessment of water-accommodated fractions from two different oils using a zebrafish (*Danio rerio*) embryo-larval bioassay with a multilevel approach. *Sci. Total Environ.* 568, 952–966. doi:10.1016/j.scitotenv.2016.04.186

Plastics Europe (2019). Plastics – The facts 2019: An analysis of European plastics production, demand and waste data. Available at: https://www.plasticseurope.org/en/resources/publications/1804-plastics-facts-2019 (accessed Oct 15, 2021).

Reichel, J., Graßmann, J., Knoop, O., Drewes, J. E., and Letzel, T. (2021). Organic contaminants and interactions with micro- and nano-plastics in the aqueous environment: Review of Analytical Methods. *Molecules* 26, 1164. doi:10.3390/molecules26041164

Rios Mendoza, L. M., Taniguchi, S., and Karapanagioti, H. K. (2017). in *Advanced analytical techniques for assessing the chemical compounds related to microplastics" in Comprehensive Analytical Chemistry*. Editors T. A. P. Rocha-Santos and A. C. Duarte (Amsterdam, The Netherlands): Elsevier), 209–240.

Shahul Hamid, F., Bhatti, M. S., Anuar, N., Anuar, N., Mohan, P., and Periathamby, A. (2018). Worldwide distribution and abundance of microplastic: How dire is the situation? *Waste Manag. Res.* 36, 873–897. doi:10.1177/0734242x18785730

Shen, M., Zhang, Y., Zhu, Y., Song, B., Zeng, G., Hu, D., et al. (2019). Recent advances in toxicological research of nanoplastics in the environment: A review. *Environ. Pollut.* 252, 511–521. doi:10.1016/j.envpol.2019.05.102

Singer, M. M., Aurand, D., Bragin, G. E., Clark, J. R., Coelho, G. M., Sowby, M. L., et al. (2000). Standardization of the preparation and quantitation of water-accommodated fractions of petroleum for toxicity testing. *Mar. Pollut. Bull.* 40, 1007–1016. doi:10.1016/s0025-326x(00)00045-x

Skrzypek, G. J., Ortega-Zamora, C., González-Sálamo, J., Hernández-Sánchez, C., and Hernández-Borges, J. (2021). The current role of chromatography in microplastic research: Plastics chemical characterization and sorption of contaminants. *J. Chromatogr. Open* 1, 100001. doi:10.1016/j.jcoa.2021.100001

Strungaru, S., Jije, R., Nicoara, M., Plavan, G., and Faggio, C. (2019). Micro-(nano) plastics in freshwater ecosystems: Abundance, toxicological impac and quantification methodology. *Trends Anal. Chem.* 110, 116–128.

Teuten, E. L., Rowland, S. J., Galloway, T. S., and Thompson, R. C. (2007). Potential for plastics to transport hydrophobic contaminants. *Environ. Sci. Technol.* 41, 7759–7764. doi:10.1021/es071737s

Wang, J., Liu, X., Liu, G., Zhang, Z., Wu, H., Cui, B., et al. (2019). Size effect of polystyrene microplastics on sorption of phenanthrene and nitrobenzene. *Ecotoxicol. Environ. Saf.* 173, 331–338. doi:10.1016/j.ecoenv.2019.02.037

Wang, W., and Wang, J. (2018a). Comparative evaluation of sorption kinetics and isotherms of pyrene onto microplastics. *Chemosphere* 193, 567–573. doi:10.1016/j.chemosphere.2017.11.078

Wang, W., and Wang, J. (2018b). Different partition of polycyclic aromatic hydrocarbon on environmental particulates in freshwater: Microplastics in comparison to natural sediment. *Ecotoxicol. Environ. Saf.* 147, 648–655. doi:10.1016/j.ecoenv.2017.09.029

Yang, K., and Xing, B. (2010). Adsorption of organic compounds by carbon nanomaterials in aqueous phase: Polanyi theory and its application. *Chem. Rev.* 110, 5989–6008. doi:10.1021/cr100059s

Yu, Y., Mo, W. Y., and Luukkonen, T. (2021). Adsorption behaviour and interaction of organic micropollutants with nano and microplastics – a review. *Sci. Total Environ.* 797, 149140. doi:10.1016/j.scitotenv.2021.149140

Zhan, Z., Wang, J., Peng, J., Xie, Q., Huang, Y., and Gao, Y. (2016). Sorption of 3, 3′, 4, 4′-tetrachlorobiphenyl by microplastics: A case study of polypropylene. *Mar. Pollut. Bull.* 210, 559–563. doi:10.1016/j.marpolbul.2016.05.036